

Article

Research on a Classification Method of Goaf Stability Based on CMS Measurement and the Cloud Matter–Element Model

Jiazhao Chen ^{1,2} , Yuye Tan ^{1,2,*} , Xu Huang ^{1,2} and Jianxin Fu ^{1,2}

¹ Key Laboratory of High-Efficient Mining and Safety of Metal Mines (Ministry of Education of China), University of Science and Technology Beijing, Beijing 100083, China; cjjgzyx2021@163.com (J.C.)

² School of Civil and Resources Engineering, University of Science and Technology Beijing, Beijing 100083, China

* Correspondence: tanyuye@ustb.edu.cn

Abstract: The evaluation and classification of goaf stability are fuzzy and random. To address this problem, a new classification method is proposed. A cavity monitoring system is used to detect the goaf, 3DMine and FLAC3D software are used to conduct the 3D visual modeling of the scanning results, and numerical simulation analysis is performed on the goaf. According to the analysis results, the stability classification standard of the goaf is constructed, and the characteristics of each classification are described. The evaluation indicator system of goaf stability is constructed in accordance with similar engineering experience, and the evaluation indicator is weighted by using the analytic hierarchy process. The cloud–element coupling evaluation model is built, the field measured values of indicators are collected, the cloud correlation degree of goafs belonging to each stability level is calculated, the stability level is evaluated according to the principle of maximum membership degree, and the results are compared with the numerical simulation to analyze the reasons for the differences in the stability evaluation results obtained by the two methods and to improve the accuracy of the evaluation of goaf stability. The pillar stress and surrounding rock deformation are monitored in Room 1# of the inclined mining area of Shirengou Iron Mine. The monitoring results are consistent with the evaluation results, which proves the accuracy of the proposed goaf stability classification method.



Citation: Chen, J.; Tan, Y.; Huang, X.; Fu, J. Research on a Classification Method of Goaf Stability Based on CMS Measurement and the Cloud Matter–Element Model. *Appl. Sci.* **2024**, *14*, 3774. <https://doi.org/10.3390/app14093774>

Received: 16 April 2024

Revised: 24 April 2024

Accepted: 24 April 2024

Published: 28 April 2024



Copyright: © 2024 by the authors. Licensee MDPI, Basel, Switzerland. This article is an open access article distributed under the terms and conditions of the Creative Commons Attribution (CC BY) license (<https://creativecommons.org/licenses/by/4.0/>).

1. Introduction

For a long time, goaf stability has been a difficult problem in the safe production of many mines. Due to the exhaustion of shallow surface minerals, the exploitation of mineral resources in China has gradually developed at greater depths. With the deepening of mining depth, numerous goafs remain. The retention of numerous goafs has seriously affected the safe production of mines [1–4]. The existence of a goaf easily causes problems such as roof collapse, surface collapse, and water inrush in the roof and floor; it also increases the difficulties and obstacles for subsequent mining construction [5–8].

Goaf stability evaluation is the assessment of goaf stability through theoretical analysis, prediction evaluation, or simulation based on a mine's geological characteristics, technical conditions, management mode, and other related factors [9,10]. Goaf stability is affected by many factors. At present, many scholars have researched goaf stability evaluation [11–19]. In existing studies, the most widely used evaluation method is the combination of prediction and simulation [20]. The commonly used prediction and evaluation method is the fuzzy comprehensive evaluation method based on the analytic hierarchy process (AHP) [21–23]. However, the classification standard of goaf stability in the traditional prediction and evaluation model is more inclined to empirical judgment, and the classification is fuzzy and subjective. Therefore, this paper proposes a method to determine the stability classification

of goafs based on the combination of cavity monitoring system (CMS) goaf detection and FLAC3D numerical simulation.

The 3D laser CMS has been applied in the stability evaluation of goafs for a long time. CMS detection is combined with 3D modeling software and numerical simulation software to evaluate a goaf, and the geological model is converted into a digital model to simulate its stability. This approach can improve the reliability of the evaluation results [24–26]. However, this method of evaluating the goaf stability directly through numerical simulation often simplifies the intermediate calculation and has difficulty matching the actual complex condition of the mine. Therefore, using CMS goaf detection and FLAC3D numerical simulation to determine the classification standard of goaf stability and employing AHP and the cloud matter-element model as prediction and evaluation models can overcome the shortcomings of traditional prediction and evaluation methods, including the subjectivity of stability and the poor accuracy of the numerical simulation methods.

Shirengou Iron Mine is taken as the engineering background to address the problem of the immense number of goafs left by house-pillar mining at the −60 m stage. CMS detection and 3DMine modeling methods are used to obtain the spatial morphology and volume characteristics of each goaf. Then, the stability is graded according to the numerical simulation results. The stability of the goaf is evaluated by AHP and the cloud matter-element model. Lastly, field monitoring is conducted to verify the accuracy of the goaf stability classification method further. To address problems such as the lack of objectivity and the one-sided evaluation of the goaf stability and classification methods in the past, this paper proposes a set of practical, feasible procedures and methods, which improves the scientificity and rationality of goaf classification evaluation and possesses satisfactory theoretical value and engineering relevance.

2. Stability Classification of Goafs Based on CMS Measurement and Numerical Simulation

2.1. General Situation of Shirengou Iron Mine Engineering Aspects Materials and Preparation

Shirengou Iron Mine is an Anshan-type magnet deposit, which began operating in July 1975. Shirengou Iron Mine adopts open-pit mining to underground mining and open-pit method to fill method to conduct mine production. Open-pit mining to underground mining is constructed in three phases. The first phase of the underground project is the area south of exploration line 16 in the middle of 0–60 m and has an annual output of 600,000 t. The mining scope of the second underground project is the area north of exploration line 16, that is, the orebody in the middle section of −16–−60 m. The mining range of the third underground project is the ore body in the middle section of −60–−210 m and has an annual output of 2 million t [27–31]. The mining area is divided into north and south mining sections by the 18th exploration line. Currently, the open-pit mining in the south area has been completed, and the internal waste dump has been filled with waste rocks to an average elevation of about 140 m.

With the implementation of underground engineering, many goafs remained inside the mine, and Shirengou Iron Mine was transferred to underground tunnel mining after 2001. During the mining of the underground tunnel, many illegal mining laneways (illegal goafs) were found. The number of goafs was unknown, causing a massive water surge and seriously endangering mine safety production. In this case, the goafs caused a great safety hazard to the production of the mine, and the stability of each goaf must be detected and evaluated, which can provide an important basis for the subsequent treatment of the mine. The composite diagram of each goaf and its 0 m roadway, −60 m roadway, and surface solid model is shown in Figure 1.

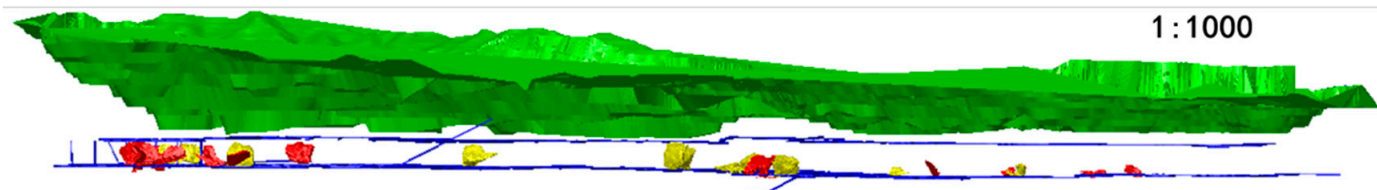


Figure 1. Composite diagram of each goaf with 0 m roadway, -60 m roadway, and surface solid model. The green part of the model in the figure represents the surface entity model, the blue part represents the roadway at 0 m and -60 m levels, and the red and yellow models represent various goafs.

2.2. Construction of 3D Solid Model of Goafs Based on CMS Detection

The 3D laser CMS is a cavity detection system for underground mines developed by Noranda Technology Center and Optech Systems. In this paper, CMS is used to detect 34 goaf areas in Shirengou Iron Mine, and each surveyed goaf area is divided into six parts according to spatial orientation, namely, south of F18 fault, between F18 and F19 faults, north end of south mining area, north branch, inclined mining area, and measure well mining area, as shown in Table 1. The detection data from the CMS for probing the goaf areas can be directly imported into 3DMine software. After solid editing and verification, solid models for each goaf area are generated. A diagram of the 3D solid models of the goaf areas is shown in Figure 2, where the positions of the goaf areas do not represent their spatial relationships.

3Dmine is used to establish a solid model of each goaf, and more accurate goaf volume can be estimated through the solid model volume estimation function of the software to prepare for the later goaf-filling work. The volume of each goaf is shown in Table 1.

The total volume of the measured goaf areas reaches $298,215 \text{ m}^3$, as shown in Table 1. Among them, 63% of the goaf volume is greater than 5000 m^3 ; under the influence of these large-volume goafs, the risk of mining is high. By combining the solid model with FLAC3D numerical simulation software, further mechanical analysis is performed to evaluate goaf stability and its influence on the mining area and to determine goaf stability and the next treatment method.

Table 1. The measured volume of each goaf area.

Block Name	Goaf Number	Volume (m^3)	Block Name	Goaf Number	Volume (m^3)
South of the F18 fault (3)	F18N-10#	2560	Measure well mining area (10)	XJ-2#	2656
	F18N-12#	998		XJ-3#	3344
	F18N-13#	1253		XJ-4#	13,670
Between F18 and F19 faults (3)	DCJ-1#	2500		XJ-7#	13,344
	DCJ-3#	2640.69		XJ-24#	16,000
	DCJ-6#	1984.38		XJ-39#	20,981
North end of south mining area (5)	NCB-3#	23,444		XJ-40#	24,274
	NCB-8#	1469		CSJ-2#	12,544
	NCB-10#	2745		CSJ-3#	5440
	NCB-17#	9008		CSJ-4#	3648
	NCB-19#	6208		CSJ-5#	7050
North branch (5)	BFZ-2#	11,594		CSJ-6#	1269
	BFZ-3#	2298		CSJ-7#	5327
	BFZ-6#	6831		CSJ-8#	12,750
	BFZ-8#	8192		CSJ-11#	12,672
Inclined shaft mining area (8)	BFZ-9#	21,304		CSJ-X#	3456
	XJ-1#	11,313		CSJ-12#	Cut through 23,448
Total 298,215.07					

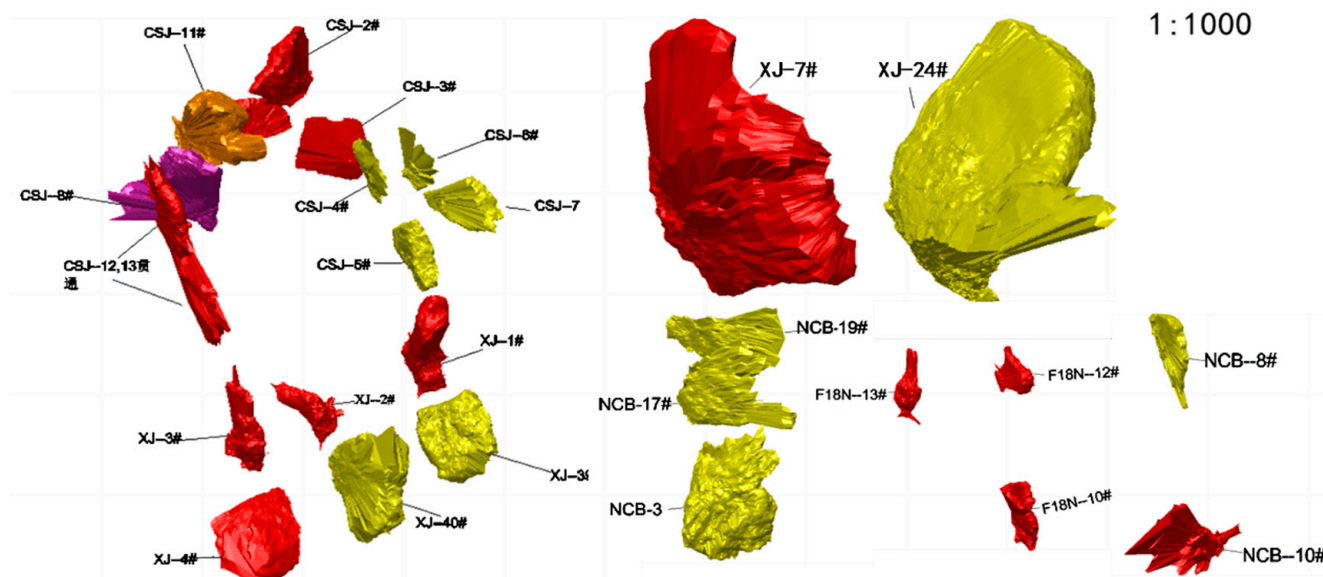


Figure 2. Three-dimensional solid model of goaf areas.

2.3. Numerical Simulation Analysis of Goaf Stability

According to the basic 3D model obtained by 3DMine, the data files of the basic model are operated and converted to obtain a mesh model that can be numerically simulated using FLAC3D. The model is assigned values with the mechanical parameters obtained onsite for simulation calculation. The surrounding rock of Shirengou iron ore body is simple, and the top and bottom of the goaf areas are biotite hornblende plagioclase gneiss and hornblende plagioclase gneiss. The specific physical and mechanical parameters of the rocks in the numerical simulation are shown in Table 2.

Table 2. Experimental data table of physical and mechanical parameters of surrounding rock.

Rock Name	Bulk Density g/cm ³	Compressive Strength MPa	Tensile Strength MPa	Shear Parameter		Deformation Parameter	
				Cohesion C MPa	Angle of Internal Friction φ	Modulus of Elasticity 10 ⁴ MPa	Poisson's Ratio
M ₁ orebody	3.58	99.44	11.95	2.183	48.36	8.03	0.21
M ₂ orebody	3.46	130.77	10.52	2.367	53.33	7.59	0.20
Biotite hornblende plagioclase gneiss	2.74	141.58	14.37	2.754	55.08	6.98	0.26

Elastic models are constructed in FLAC3D to simulate the displacement, stress, and distribution of the plastic zone of each goaf under various conditions. Goaf CSJ-2# is selected as an example in Table 2. Numerical simulation diagrams of the displacement, plastic zone, and the minimum and maximum principal stress of goaf CSJ-2# are presented in Figures 3–6.

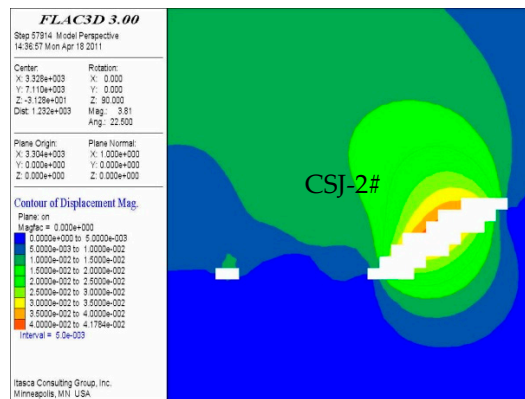


Figure 3. CSJ-2# goaf displacement cloud map.

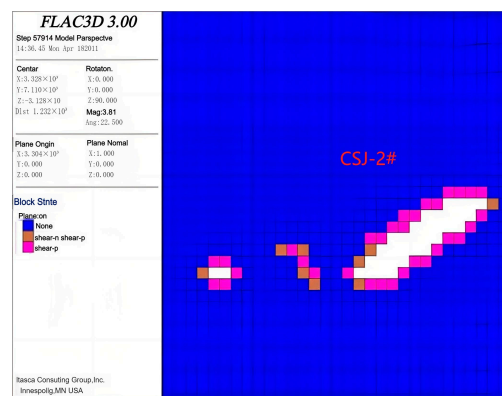


Figure 4. CSJ-2# goaf plastic zone distribution.

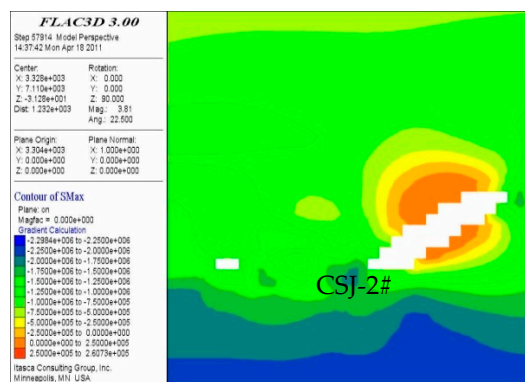


Figure 5. Minimum principal stress in goaf CSJ-2#.

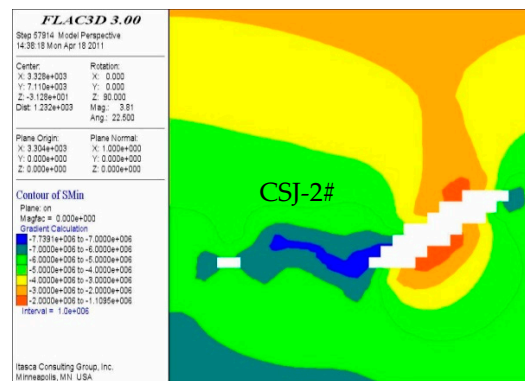


Figure 6. Maximum principal stress in goaf CSJ-2#.

Figure 3 is the goaf displacement cloud map, which shows that the maximum displacement is in the middle part of the goaf on the upper wall, with a size of 4.2 cm. Figure 4 shows the layout of plastic differentiation in the goaf. A plastic zone exists in the surrounding rock of the goaf and at the bottom of the goaf upper wall. Figures 5 and 6 show the cloud map of the maximum and minimum principal stresses of the goaf. The minimum principal stress at the roof position of goaf CSJ-2# is 0.25 MPa, which is the tensile stress. The maximum principal stress is 7.74 MPa in the lower part of the left goaf wall, and the maximum principal stress of the roof is 7.00 MPa.

According to the numerical simulation analysis results of the goaf areas in Shirengou, the maximum displacement of the goaf roof, the maximum lateral displacement of the goaf side wall or pillar, and the minimum principal stress of the goaf roof are measured, and the final statistical results are shown in Figure 7.

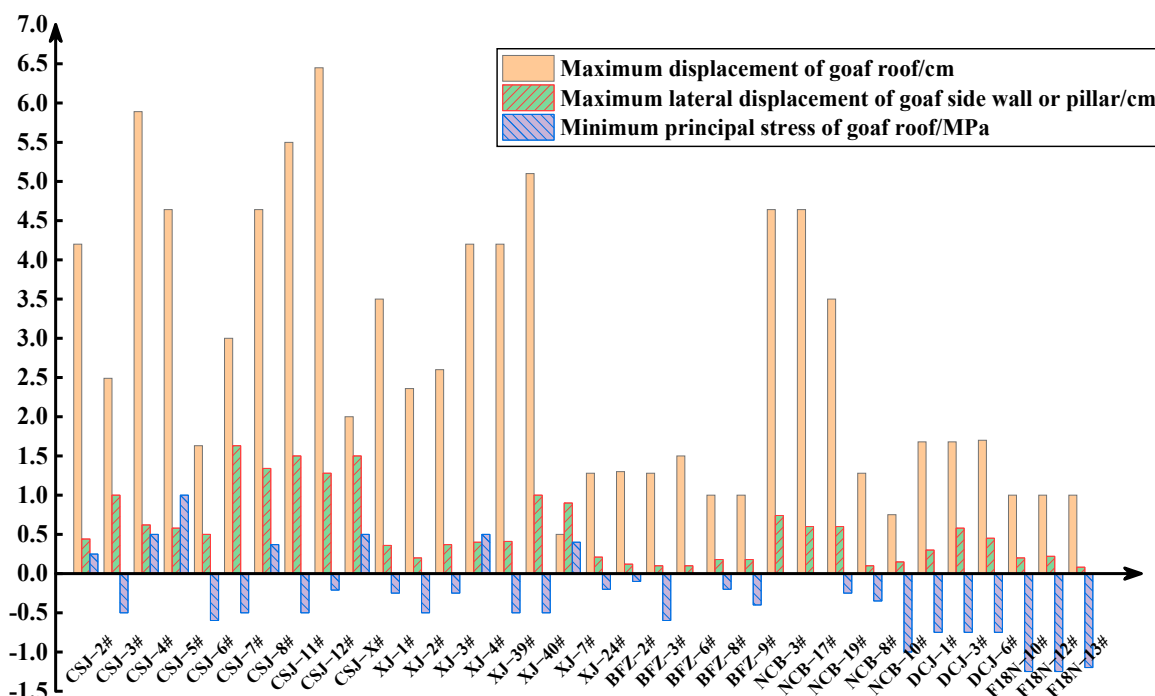


Figure 7. Statistical chart of numerical simulation results.

According to the analysis in Figure 7, the displacement of the goaf roof and side wall in the stope area of the measure well is large because the goaf distribution in this area is very dense, forming a group effect, and they influence each other to increase their respective displacements. In addition, the roof displacement of goafs with a larger span is larger. Moreover, the goaf roof tensile stress is concentrated in the stope of the measure well, which indicates that the goaf group effect has a major influence on goaf stability. The lateral displacement of the goaf side wall and pillar is small, which suggests that the pillar or side wall is stable.

The simulation results reveal that the stability of the goaf can be described, the corresponding risk degree of the goaf can be obtained from the description, and the stability level can be defined to explain the stability of the goaf. The numerical simulation analysis reveals the stability grade is divided into three levels: I (stable), II (locally unstable), and III (unstable). Table 3 summarizes this goaf stability classification.

Table 3. Goaf stability classification summary table.

Goaf Stability Level	Number of Goafs	Goaf Characteristics
I	10 (29.4%)	The goaf roof displacement is small, the goaf is relatively independent, and the distance from other goafs is far, the plastic zone of surrounding rock is less, the stress is less, and the distance from illegal goafs is far.
II	14 (38.2%)	The goaf roof displacement is large, and the distance between the goaf and the surrounding goafs is relatively close, but the goaf density in the area is small, the surrounding rock plastic zone is more, and the roof or pillar area is connected with other goaf plastic zones. The stress state of the roof is close to the tensile stress zone, and the pillar stress is larger.
III	10 (29.4%)	The goaf roof displacement is large, the stress state of the roof is poor, local tensile stress occurs, the goaf density in the area is large, the interaction between the goaf, the plastic zone of surrounding rock, and pillar is huge, and a large area of horizontal diffusion and penetration occurs, and it is greatly affected by illegal goafs.

2.4. Stability Evaluation Based on Numerical Simulation Analysis

The results of numerical simulation and the description of stability classification reveal the stability classification of each goaf. The stability classification mainly depends on the stress and displacement of surrounding rock during excavation and the distribution of plastic zone caused by it. Table 4 presents the stability ratings of each goaf based on the numerical simulation results.

Table 4. Stability rating of each goaf.

Goaf Stability Level	I	II	III
Goaf number	XJ-3#, XJ-7#, BFZ-2#, BFZ-3#, NCB-8#, NCB-10#, DCJ-1#, DCJ-6#, F18N-12#, F18N-13#	CSJ-3#, CSJ-6#, CSJ-7#, XJ-1#, XJ-2#, XJ-39#, XJ-24#, BFZ-6#, BFZ-8#, BFZ-9#, NCB-3#, NCB-19#, DCJ-3#, F18N-10#	CSJ-2#, CSJ-4#, CSJ-5#, CSJ-8#, CSJ-11#, CSJ-12#, CSJ-X#, XJ-4#, XJ-40#, NCB-17#

The classification results show that 10 goaf are in a stable state, 14 are in a local unstable state, and 10 are in an unstable state. The goafs in the unstable state are concentrated in the measure well and the north end of the south mining area. The main feature is that the density of these goafs is exceptionally large, and a group effect is observed between the goafs, which reduces the stability level of each goaf.

3. Goaf Stability Evaluation Based on the Cloud Matter–Element Model

3.1. Construction of the Cloud Matter–Element Model Based on AHP

Figure 8 shows that to evaluate the stability of a goaf, first, a stability evaluation indicator system must be built, the classification standard and weight of each indicator must be determined, a cloud matter–element model must be established, and the stability level of the goaf must be calculated.

The weighting method in this paper is AHP, which is a subjective weighting method based on the experience of decision makers, a practical multicriteria decision-making method, and a comprehensive evaluation method combining qualitative and quantitative methods [32–34]. The weights obtained are used in the calculation of the cloud matter–element model. In this study, we invited two experienced professors to participate in the weighting process of the AHP and assign scores to the indicators.

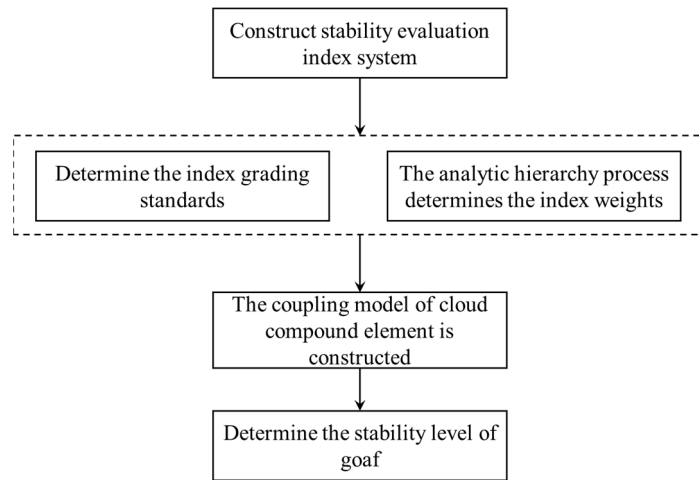


Figure 8. The stability evaluation method of cloud compound meta-model.

The cloud matter-element model is a combination of cloud model and matter-element theory. Matter-element analysis mainly uses the three elements of the thing, name J , feature K , and the corresponding quantity value L , to express things in the form of ordered triples. This triplet is called matter-element and is denoted as $R = (J, K, L)$. The cloud matter-element model uses the digital features of the cloud model to replace the feature quantity value L to build the cloud compound element model [35], as shown in Equation (1).

$$R = (J, K, L) = \begin{pmatrix} J & K_1 & (E_{x_1}, E_{n_1}, H_{e_1}) \\ & K_2 & (E_{x_2}, E_{n_2}, H_{e_2}) \\ & \vdots & \vdots \\ & K_n & (E_{x_n}, E_{n_n}, H_{e_n}) \end{pmatrix} \quad (1)$$

E_x is the expected value, which is the central value at the center of the domain. E_n is the entropy, which is a measure of the ambiguity of qualitative concepts, and represents the range of all possible values in the discourse domain. The larger the entropy is, the larger the range is, and the stronger the fuzziness is. H_e is the entropy of E_n , which represents the dispersion degree of cloud droplets in the cloud model and indirectly reflects the thickness of the cloud.

$$E_x = \frac{d_{\min} + d_{\max}}{2} \quad (2)$$

$$E_n = \frac{d_{\max} - d_{\min}}{6} \quad (3)$$

$$H_e = k \quad (4)$$

d_{\max} and d_{\min} are the maximum and minimum values of the value range of evaluation indicators, respectively. k is a constant, which is determined according to the fuzziness and randomness of the evaluation of goaf stability. In this paper, 0.02 is adopted [18]. According to the obtained cloud digital characteristics and the standardized values of each indicator, the cloud correlation degree between each indicator and the cloud model is calculated by Equation (5).

$$t = \exp \left[-\frac{(x - E_x)^2}{2(E_n)^2} \right] \quad (5)$$

3.2. Determining the Grading Standards and Weights of Evaluation Indicators

The deformation and failure of a goaf is always produced under the action of several specific influencing factors, and each influencing factor is composed of several factors. According to existing research results on the influencing factors of goaf stability and the

understanding of the actual situation of a goaf, the goaf stability evaluation indicator system is constructed by selecting four indicators including hydrogeological factors, rock strength factors, goaf parameters, and other factors. The goaf stability indicator system is shown in Figure 9.

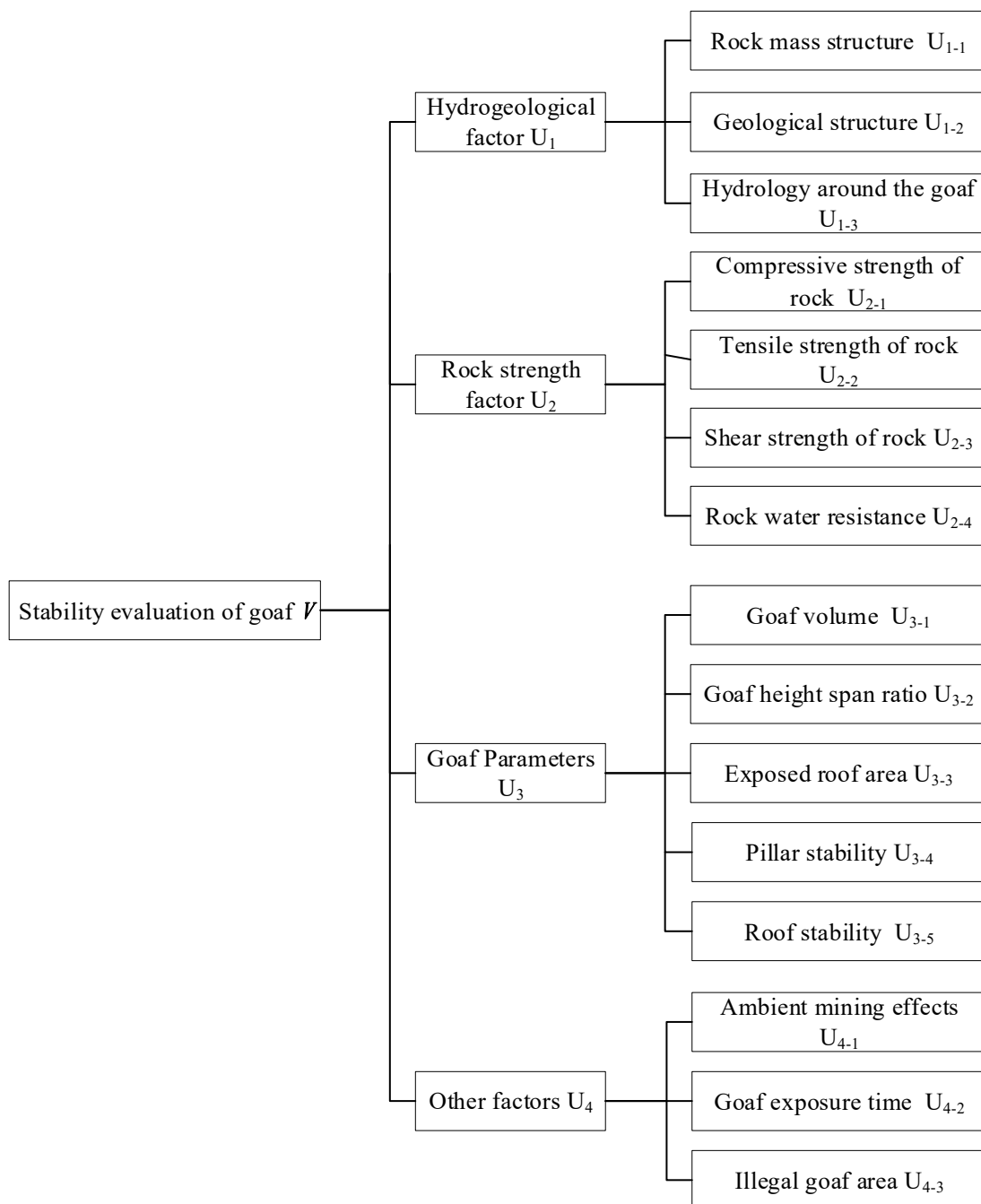


Figure 9. Goaf stability indicator system.

According to the stability classification standard measured by CMS and the description of different stability levels, each factor is divided into three levels, and the qualitative indicators are quantified with a score system of 0–1 and then graded. The grading standards for indicators are determined by referencing the descriptions of goaf stability classification in the preceding text as well as practical engineering experience. The classification standard of goaf stability evaluation indicators is shown in Table 5.

Table 5. Evaluation indicator grading standard of goaf stability.

Evaluation Intermediate Layer	Evaluation Factor Layer	Stable (Level I)	Locally Unstable (Level II)	Unstable (Level III)
Hydrogeological factor U ₁	Rock mass structure U ₁₋₁	(0.66, 0.99]	(0.33, 0.66]	[0, 0.33]
	Geological structure U ₁₋₂	[0, 5]	(5, 15]	(15, 30]
	Hydrology around the goaf U ₁₋₃	(0.66, 0.99]	(0.33, 0.66]	[0, 0.33]
Rock strength factor U ₂	Compressive strength of rock U ₂₋₁	(40, 80]	(20, 40]	[0, 20]
	Tensile strength of rock U ₂₋₂	(2.5, 6]	(1, 2.5]	[0, 1]
	Shear strength of rock U ₂₋₃	(45, 60]	(30, 45]	[0, 30]
	Rock water resistance U ₂₋₄	(0.75, 0.9]	(0.5, 0.75]	[0, 0.5]
Goaf parameters U ₃	Goaf volume U ₃₋₁	[0, 3000]	(3000, 6000]	(6000, 10,000]
	Goaf height-span ratio U ₃₋₂	(0.87, 1.17]	(0.75, 0.87]	[0, 0.75]
	Exposed roof area U ₃₋₃	[0, 500]	(500, 1000]	(1000, 1500]
Other factors U ₄	Pillar stability U ₃₋₄	(0.66, 0.99]	(0.33, 0.66]	[0, 0.33]
	Roof stability U ₃₋₅	(0.66, 0.99]	(0.33, 0.66]	[0, 0.33]
	Ambient mining effects U ₄₋₁	(0.66, 0.99]	(0.33, 0.66]	[0, 0.33]
	Goaf exposure time U ₄₋₂	[0, 30]	(30, 50]	(50, 100]
	Illegal goaf area U ₄₋₃	(0.66, 0.99]	(0.33, 0.66]	[0, 0.33]

After determining the grading standards of each indicator, the indicator weight vector is calculated as $W = (0.121 \ 0.275 \ 0.032 \ 0.039 \ 0.013 \ 0.039 \ 0.013 \ 0.018 \ 0.183 \ 0.085 \ 0.050 \ 0.091 \ 0.011 \ 0.028 \ 0.005)^T$ based on AHP. This weight vector is the final result of AHP.

3.3. Stability Classification Based on the Cloud Matter–Element Model

According to the current detection results, each detected goaf is widely distributed, and each goaf has a different morphology and hydrogeological environment; thus, each goaf must be evaluated separately, taking the stability evaluation of BFZ-8# goaf as an example. The data of each evaluation indicator of goaf BFZ-8# are shown in Table 6. The qualitative indicator is standardized, whereas the quantitative indicator retains the original data.

Table 6. Evaluation indicator data of goaf BFZ-8#.

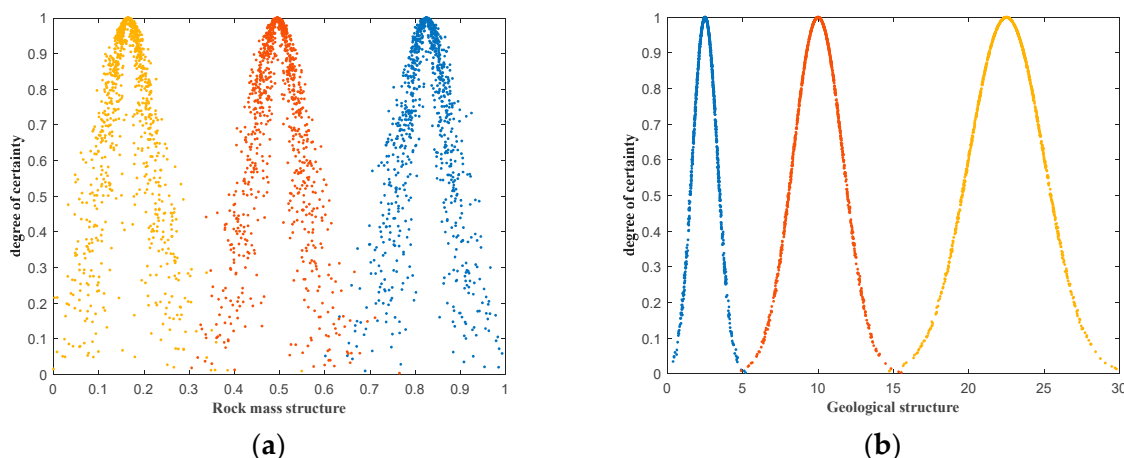
Indicator	Measured Value	Standardized Data
Rock mass structure U ₁₋₁	The surrounding rock inside the void zone is broken and complicated.	0.3
Geological structure U ₁₋₂	5.0	0.5
Hydrology around the goaf U ₁₋₃	There is less water around the empty area.	0.88
Compressive strength of rock U ₂₋₁	80	80
Tensile strength of rock U ₂₋₂	6	6
Shear strength of rock U ₂₋₃	60	60
Rock water resistance U ₂₋₄	0.75	0.75
Goaf volume U ₃₋₁	12,264	12,264
Goaf height-span ratio U ₃₋₂	0.78	0.78
Exposed roof area U ₃₋₃	408.8	408.8
Pillar stability U ₃₋₄	The pillar meets the design requirements and is stable without damage.	0.99
Roof stability U ₃₋₅	Instability.	0.3
Ambient mining effects U ₄₋₁	There is no mining activity around the goaf, and the disturbance is less.	0.9
Goaf exposure time U ₄₋₂	150	150
Illegal goaf area U ₄₋₃	The surrounding illegal goaf area is relatively far.	0.5

MATLAB is used to calculate the three cloud digital features of each index cloud model according to Equations (2)–(4), and the random number E'_n is obtained, as shown in Table 7, which is the data basis for the next calculation of cloud correlation degree. The normal cloud map of rock mass structure, geological structure, goaf height–span ratio, and goaf volume, which are four factors that greatly influence goaf stability, is drawn, as shown in Figure 7.

Table 7. Evaluation index cloud digital characteristics of goaf BFZ-8#.

Indicator	Stable (I)		Locally Unstable (II)		Unstable (III)	
	Digital Feature	E'_n	Digital Feature	E'_n	Digital Feature	E'_n
U ₁₋₁	(0.825, 0.055, 0.02)	0.0558	(0.495, 0.055, 0.02)	0.0553	(0.165, 0.055, 0.02)	0.0605
U ₁₋₂	(2.5, 0.833, 0.02)	0.8069	(10, 1.667, 0.02)	1.6029	(22.5, 2.5, 0.02)	2.5234
U ₁₋₃	(0.825, 0.055, 0.02)	0.0533	(0.495, 0.055, 0.02)	0.0651	(0.165, 0.055, 0.02)	0.0336
U ₂₋₁	(60, 6.667, 0.02)	6.6882	(30, 3.333, 0.02)	3.3122	(10, 3.333, 0.02)	3.3213
U ₂₋₂	(4.25, 0.583, 0.02)	0.5525	(1.75, 0.25, 0.02)	0.2918	(0.5, 0.167, 0.02)	0.1832
U ₂₋₃	(52.5, 2.5, 0.02)	2.4934	(37.5, 2.5, 0.02)	2.4773	(15, 5, 0.02)	4.9583
U ₂₋₄	(0.825, 0.025, 0.02)	0.0264	(0.625, 0.042, 0.02)	0.0102	(0.25, 0.083, 0.02)	0.0593
U ₃₋₁	(1500, 500, 0.02)	499.9874	(4500, 500, 0.02)	500.0322	(8000, 666.667, 0.02)	666.6615
U ₃₋₂	(1.02, 0.05, 0.02)	0.0621	(0.81, 0.02, 0.02)	0.0349	(0.375, 0.125, 0.02)	0.1301
U ₃₋₃	(250, 83.333, 0.02)	83.3330	(750, 83.333, 0.02)	83.3176	(1250, 83.333, 0.02)	83.3355
U ₃₋₄	(0.825, 0.055, 0.02)	0.0576	(0.495, 0.055, 0.02)	0.0846	(0.165, 0.055, 0.02)	0.0685
U ₃₋₅	(0.825, 0.055, 0.02)	0.0731	(0.495, 0.055, 0.02)	0.0424	(0.165, 0.055, 0.02)	0.0447
U ₄₋₁	(0.825, 0.055, 0.02)	0.0600	(0.495, 0.055, 0.02)	0.0377	(0.165, 0.055, 0.02)	0.0540
U ₄₋₂	(15, 5, 0.02)	5.0232	(40, 3.333, 0.02)	3.3411	(75, 8.333, 0.02)	8.3496
U ₄₋₃	(0.825, 0.055, 0.02)	0.0566	(0.495, 0.055, 0.02)	0.0334	(0.165, 0.055, 0.02)	0.0550

Figure 10 shows that the cloud thickness of rock mass structure and goaf height-span ratio is large, which means that the dispersion degree of indicators is high, and the membership degree obtained by the cloud model is more random. The cloud thickness of geological structure and void volume is low, the degree of dispersion is small, and the randomness of membership is smaller. For the index with strong membership randomness, 10 random numbers are weighted to determine the final membership. According to the cloud digital features in Table 7, random number E'_n , and Equation (5), the cloud correlation matrix Z is calculated by MATLAB, as shown in Table 8 below.

**Figure 10. Cont.**

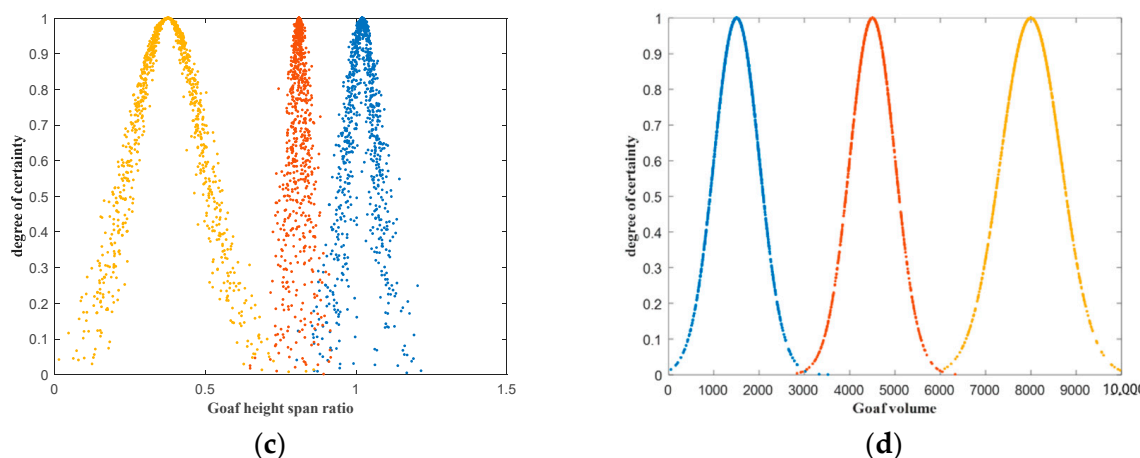


Figure 10. (a) Rock mass structure normal cloud map; (b) geological structure normal cloud map; (c) goaf height–span ratio normal cloud map; (d) goaf volume normal cloud map.

Table 8. Goaf evaluation index corresponds to grade cloud correlation degree.

Goaf Stability Level	Stable (I)	Locally Unstable (II)	Unstable (III)
U ₁₋₁	0.0000	0.0020	0.0829
U ₁₋₂	0.0463	0.0000	0.0000
U ₁₋₃	0.5872	0.0000	0.0000
U ₂₋₁	0.0114	0.0000	0.0000
U ₂₋₂	0.0066	0.0000	0.0000
U ₂₋₃	0.0108	0.0000	0.0000
U ₂₋₄	0.0177	0.0000	0.0000
U ₃₋₁	0.0000	0.0000	0.0000
U ₃₋₂	0.0006	0.6911	0.0079
U ₃₋₃	0.1627	0.0002	0.0000
U ₃₋₄	0.0165	0.0000	0.0000
U ₃₋₅	0.0000	0.0000	0.0105
U ₄₋₁	0.4578	0.0000	0.0000
U ₄₋₂	0.0000	0.0000	0.0000
U ₄₋₃	0.0000	0.9889	0.0000

The calculated weight vector W and cloud correlation matrix Z can be substituted into Equation (6) to determine the membership vector $G = (0.0525, 0.1317, 0.0124)$. According to the principle of maximum membership, the stability of the goafs of BFZ-8# belongs to level II and is in a locally unstable state.

$$G = W \cdot Z \quad (6)$$

The evaluation results are verified by the actual field investigation, and the results are consistent with the actual situation of the project. This outcome shows that the selection of indicators and the weights of each factor and factor are scientific, this method can be applied to perform the same calculation on other goafs in Shirengou, and the stability evaluation results can be compared with the numerical simulation results, as shown in Table 9, which is a comparison between the two evaluation results of numerical simulation analysis and the cloud matter-element model.

Table 9. Comparison of the results of two evaluation methods.

Goaf Number	Stability Level	Numerical Simulation Analysis Level	Final Level	Goaf Number	Stability Level	Numerical Simulation Analysis Level	Final Level
CSJ-2#	III	III	III	XJ-24#	II	II	II
CSJ-3#	III	II	III	BFZ-2#	II	I	II
CSJ-4#	III	III	III	BFZ-3#	I	I	I
CSJ-5#	III	III	III	BFZ-6#	III	II	III
CSJ-6#	II	II	II	BFZ-8#	II	II	II
CSJ-7#	II	II	II	BFZ-9#	III	II	III
CSJ-8#	III	III	III	NCB-3#	III	II	III
CSJ-11#	III	III	III	NCB-17#	III	III	III
CSJ-12#	III	III	III	NCB-19#	II	II	II
CSJ-X#	III	III	III	NCB-8#	I	I	I
XJ-1#	II	II	II	NCB-10#	I	I	I
XJ-2#	II	II	II	DCJ-1#	II	I	II
XJ-3#	II	I	II	DCJ-3#	III	II	III
XJ-4#	III	III	III	DCJ-6#	II	I	II
XJ-39#	III	II	III	F18N-10#	III	II	III
XJ-40#	III	III	III	F18N-12#	II	I	II
XJ-7#	I	I	I	F18N-13#	II	I	II

The goaf stability evaluation results obtained by the two evaluation methods have a high degree of agreement, as shown in Table 9. Some goafs are graded differently by the two evaluation methods, which shows that the evaluation result of the cloud matter–element model is lower than that of the numerical simulation evaluation. The main reasons are the group effect formed by the large density of goafs in this area, the severe damage of the surrounding rock of the goafs, and the poor geological conditions of the mining area. The prediction and evaluation model comprehensively considers these factors, whereas the numerical simulation mainly performs evaluation according to the distribution of stress, displacement, and plastic zone. This approach ignores these necessary factors and results in a higher evaluation grade than the numerical simulation. Therefore, based on the rating of the cloud matter–element model and combined with the numerical simulation analysis results, the comprehensive evaluation is conducted to increase the accuracy of evaluating the goaf stability.

4. Stability Evaluation and Comparative Analysis of Goafs Based on Field Monitoring

Field monitoring is the field verification of the goaf stability level based on the previous stability evaluation results, and the results of field monitoring form the performance of the overall stability of a region. The influence of mining on goaf stability must be considered in field monitoring work, so a mining section with frequent mining activities must be selected to arrange the monitoring points. Considering the safety of the measuring points, in our study the inclined mining area with better stability evaluation results was selected as the field monitoring area. After underground field investigation, the inclined shaft mining area XJ-1# was selected as the field monitoring area.

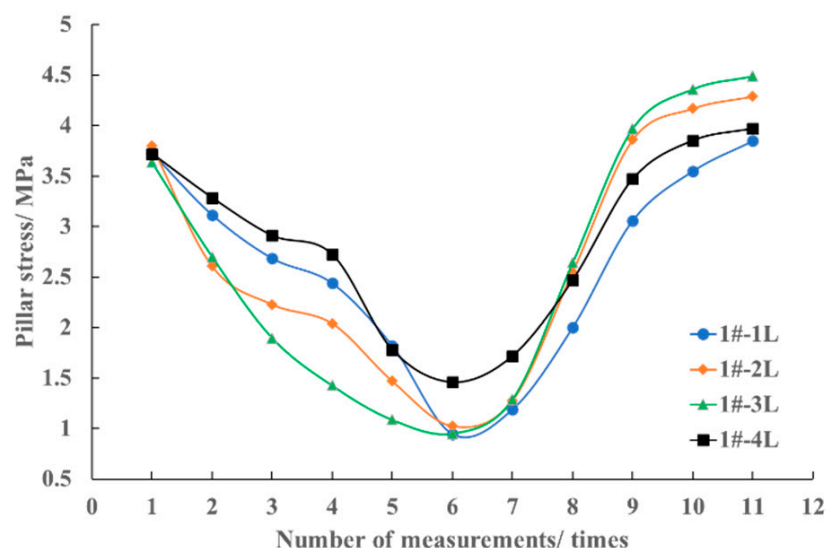
4.1. Pillar Stress Monitoring and Analysis

Four monitoring points, 1#-1L, 1#-2L, 1#-3L, and 1#-4L, were arranged on the pillar of 1# chamber in the inclined mining area by using a KSE-II-1 borehole stress meter. From the installation of the stress meter to the completion of the monitoring, 11 measurements were made, and the time span was 10 months, which reflects the stress data of the pillar during mining. The sampling data of the stress meter are shown in Table 10.

Table 10. Comparison of the results of two evaluation methods.

Sampling Number	Sampling Time	Sampling Value	Stress 1	Stress 2	Stress 3	Stress 4
1	5 September 2010	P	3.731	3.798	3.635	3.721
2	16 September 2010	P	3.117	2.608	2.702	3.285
3	30 September 2010	P	2.686	2.230	1.897	2.911
4	11 November 2010	P	2.439	2.041	1.426	2.723
5	21 January 2011	P	1.818	1.470	1.087	1.780
6	25 February 2011	P	0.944	1.025	0.952	1.46
7	23 March 2011	P	1.19	1.28	1.29	1.72
8	22 April 2011	P	2.00	2.55	2.64	2.47
9	24 May 2011	P	3.06	3.86	3.97	3.47
10	25 June 2011	P	3.55	4.17	4.36	3.85
11	25 July 2011	P	3.85	4.29	4.49	3.97

Figure 11 is the trend diagram of the data obtained from the four stress gauges. According to the analysis of stress monitoring data, the stress of horizontal surrounding rock is 1–2 MPa. With the increase of mining height, pillar stress begins to increase gradually and becomes stable near the end of mining. Generally, the surrounding rock of the roadway of Shirengou Iron Mine has satisfactory stability and a smooth stress curve.

**Figure 11.** Stress monitoring data trend chart.

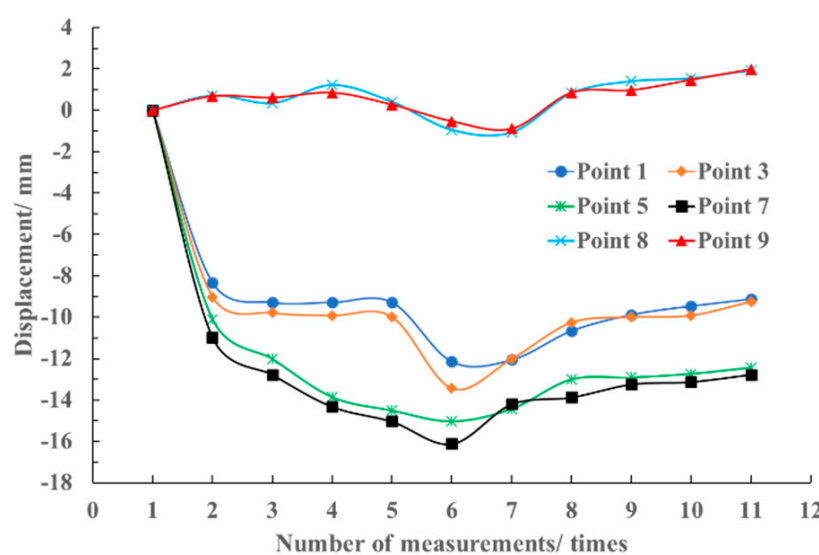
4.2. Monitoring and Analysis of Surrounding Rock Deformation

We conducted surrounding rock deformation monitoring using both a commercially available steel ruler with a precision of 0.5 mm as a multi-point displacement meter and the JSS30A digital convergence meter produced by Beijing ZhongCoal Mining Engineering Co., Ltd. Six displacement monitoring points, N18-1#, N17-1#, along vein-1#, along vein-3#, main lane-1#, and main lane-2# around mine 1#, were selected for measurement and are represented by points 1, 3, 5, 7, 8, and 9, respectively. The displacement data of six monitoring points are shown in Table 11.

Table 11. Displacement monitoring point data sheet.

Sampling Number	Sampling Time	Point 1	Point 3	
2	5 September 2010	2.5 m + 13.67 mm	2.5 m + 12.98 mm	
3	16 September 2010	2.5 m + 12.72 mm	2.5 m + 12.12 mm	
4	30 September 2010	2.5 m + 12.72 mm	2.5 m + 12.09 mm	
5	11 November 2010	2.5 m + 12.72 mm	2.5 m + 12.02 mm	
6	21 January 2011	2.5 m + 9.25 mm	2.5 m + 8.56 mm	
7	25 February 2011	2.5 m + 9.94 mm	2.5 m + 9.99 mm	
8	23 March 2011	2.5 m + 11.34 mm	2.5 m + 11.75 mm	
9	22 April 2011	2.5 m + 12.12 mm	2.5 m + 12.01 mm	
10	24 May 2011	2.5 m + 12.54 mm	2.5 m + 12.09 mm	
11	25 June 2011	2.5 m + 12.88 mm	2.5 m + 12.76 mm	
Sampling Number	Point 5	Point 7	Point 8	Point 9
2	3.5 m + 12.89 mm	3.5 m + 13.02 mm	7.575 m + 6.72 mm	5.20 m + 8.68 mm
3	3.5 m + 10.98 mm	3.5 m + 11.23 mm	7.575 m + 6.35 mm	5.20 m + 8.61 mm
4	3.5 m + 9.13 mm	3.5 m + 9.68 mm	7.575 m + 7.23 mm	5.20 m + 8.85 mm
5	3.5 m + 8.48 mm	3.5 m + 8.96 mm	7.575 m + 6.41 mm	5.20 m + 8.27 mm
6	3.5 m + 7.96 mm	3.5 m + 7.88 mm	7.575 m + 5.05 mm	5.2 m + 7.47 mm
7	3.5 m + 8.56 mm	3.5 m + 9.80 mm	7.575 m + 4.93 mm	5.25 m + 7.11 mm
8	3.5 m + 9.99 mm	3.5 m + 10.13 mm	7.575 m + 6.83 mm	5.20 m + 8.85 mm
9	3.5 m + 10.08 mm	3.5 m + 10.76 mm	7.575 m + 7.41 mm	5.20 m + 8.97 mm
10	3.5 m + 10.26 mm	3.5 m + 10.88 mm	7.575 m + 7.55 mm	5.2 m + 9.47 mm
11	3.5 m + 10.56 mm	3.5 m + 11.23 mm	7.575 m + 7.93 mm	5.25 m + 9.98 mm

The resulting data graph is shown in Figure 12. According to the monitoring data of strain, the stress of the pillar changes sharply during mining and bears the main stress; moreover, the horizontal displacement and the deformation are evident. The change of the displacement monitoring points on both sides of the mine is smaller than that of the pillar, which indicates that the disturbance of the mining room on both sides is less than that of the pillar. The change of the displacement monitoring points on the main roadway is the least, which indicates that the disturbance of the main roadway is less. Overall, the rock displacement changes slightly and stabilizes with the progress of mining, which indicates that the whole goaf is in a stable state.

**Figure 12.** Strain monitoring data diagram.

4.3. Analysis of Goaf Stability Classification Results

The analysis of stress-and-strain monitoring data of the pillar and surrounding rock of 1# mine in the inclined mining area shows that the pillar stress changes greatly during mining, but it is in a stable state before and after mining; moreover, the stress change curve is smooth, which indicates that the surrounding rock is in a satisfactory condition. The displacement of the pillar and roadway changes slightly and gently with the modification of stress, which indicates that the 1# mining room in the inclined mining area is in a safe state. The monitoring results can reflect that the overall stability of the inclined mining area is satisfactory, which is consistent with the overall stability of the inclined mining area in the prediction and evaluation results. This outcome proves that the goaf stability classification constructed in this paper is scientific and practical.

5. Conclusions

(1) The specific conditions of the goafs in the Shirengou Iron Mine are summarized, highlighting the significance of evaluating the mine's stability. CMS is utilized for goaf detection, while 3DMine and FLAC3D models are constructed for numerical simulation analysis. Goaf stability is categorized into three grades: I-level (stable), II-level (locally unstable), and III-level (unstable), with clear grading criteria established for preliminary stability evaluations.

(2) An evaluation index system for goaf stability is established, with grading standards determined for each index based on the established goaf stability grades. AHP is employed to assign weights to the indicators, and a coupled cloud matter-element model is constructed to assess the stability level of each goaf. The reasons for any discrepancies are explored through comparisons with the results of numerical simulation evaluations.

(3) Field monitoring of XJ-1# in the inclined mining area of the Shirengou Iron Mine provides insights into the stress-and-strain conditions of its pillars and surrounding rock. The analysis reveals that XJ-1# maintains a stable state throughout the mining process, indicating satisfactory stability in the inclined mining area and aligning with prediction and evaluation results. This validates the effectiveness and practicality of this goaf stability classification method, which combines CMS measurements with the cloud matter-element model.

Author Contributions: Conceptualization, X.H. and J.F.; Methodology, J.C. and Y.T.; Visualization, J.C.; Writing—original draft, J.C.; Writing—review & editing, J.C. and Y.T. All authors have read and agreed to the published version of the manuscript.

Funding: This research was funded by the National Natural Science Foundation of China [52274110], National Key Research and Development Program of China (2022YFC2905003), the Growth Program for Young Teachers at Beijing University of Science and Technology (QNXM20220004), the National Natural Science Foundation of China [52004019], the China Scholarship Council fund (202206465005).

Data Availability Statement: The data presented in this study are available on request from the corresponding author.

Conflicts of Interest: The authors declare that they have no conflicts of interest.

References

1. Sun, G.Y.; Zhang, W.Z.; Kang, Q.R.; Xia, Y.D.; Yuan, W.; Hu, Q.Z. Goaf Stability Analysis Based on Accurate 3D Laser Detection Combined with Visual Modeling. *Sci. Technol. Eng.* **2022**, *22*, 14683–14690.
2. Yuan, D.L.; He, L.; Ren, L.W.; Tian, D.P.; Dun, Z.L. Study on Influencing Factors of Goaf Stability Based on DEMATEL-ISM. *Coal Technol.* **2023**, *42*, 5–8.
3. Ren, H.G.; Wang, X.G.; Tan, Z.U.; Xia, Z.Y. Construction of three-dimensional mechanical model for creep and catastrophe of goaf group and accurate prediction of its stability. *J. Cent. South Univ. (Sci. Technol.)* **2019**, *50*, 3114–3126.
4. Zhao, L.L.; Wang, L.; Hou, Q.Y.; Wan, Z.S.; Guo, Q.B. Stability Evaluation of Construction Site above a Goaf Based on PCA-RA and Cloud Model. *Met. Mine* **2022**, *3*, 197–204.
5. Guo, M.Y.; Ding, X.N.; Xu, X.J. Application of Roadway Seismic Wave Method in the Detection of Goaf in Metal Mine. *Sci. Technol. Eng.* **2022**, *22*, 10003–10011.

6. Dong, J.J.; Zhang, Y.; Li, X.; Mei, Y. InSAR deformation monitoring and safety and stability evaluation on surface of coal mine goaf. *China Saf. Sci. J.* **2024**, *34*, 140–149.
7. Wang, S.L.; Qi, W.B.; Hao, L.H.; Lu, L.S.; Huang, M. Study on the Goaf Stability Under the Coupling Action of Complex Goaf and Pillars in Multiple Levels. *Min. Res. Dev.* **2020**, *40*, 54–59.
8. Wan, D.L.; He, L.; Huang, M.; Ren, L.W. Study on Influencing Factors of Foundation Grouting Treatment in High-speed Railway Goaf Based on Fuzzy DEMATEL-ISM. *Met. Mine* **2023**, *1*, 172–180.
9. Zhou, Y.W.; Zhang, T.; Duan, L.C.; Li, J.W. Summary of Research on Comprehensive Treatment of Mine Goaf in China. *Saf. Environ. Eng.* **2022**, *29*, 220–230.
10. Liu, X.P. Progress in investigation technology for coal mine goafs under buildings and structures in China. *Coal Geol. Explor.* **2022**, *52*, 139–146.
11. Xie, W.; Ni, S.; Li, Q.L.; Wang, L.; Wang, X.; Dai, B.B. Stability Analysis of Goaf Based on Mathews Graphic Method. *Met. Mine* **2022**, *6*, 40–45.
12. Yang, Y.; Zhang, M.S.; Zhang, F.; Hu, G.J. Stability of Complex Lead Mined-out Area of An Polymetallic Mine in Hongling. *Sci. Technol. Eng.* **2021**, *21*, 14982–14987.
13. Cai, Y.; Deng, G.L.; Zhen, L.B.; Cheng, Q.; Huang, J.Y. Mechanical Model Analysis of Goaf Considering Pillar Rheological Effect. *Met. Mine* **2022**, *2*, 96–101.
14. Luo, Z.Q.; Yang, B.; Liu, X.M.; Lu, G.; Lu, H. Stability Analysis for Goaf Group Based on CMS and Coupling of Midas-FLAC3D. *Min. Metall. Eng.* **2010**, *30*, 1–5.
15. Ke, L.H.; Meng, Y.Y.; Yao, N.; Wang, Q.H.; Tang, H.Q. Evaluation of goaf stability based on fuzzy statistical method. *China Saf. Sci. J.* **2023**, *33*, 59–67.
16. Liu, Y.; Li, K.G.; Li, M.L.; Qin, Q.C.; Ma, X.B. Study on the Stability of Mined-out Area Based on AHP-fuzzy Evaluation. *Nonferrous Met. Eng.* **2020**, *10*, 114–119.
17. Qi, Y.; Wang, W.; Liu, J.; Ge, J.Q.; Zhou, B.Q.; Zhang, M.H.; Qi, Q.J. Improved Combination Weight Coupled SPA Evaluation Model of Goaf Surrounding Rock Stability. *Met. Mine* **2022**, *12*, 23–29.
18. Zhang, G.J.; Quan, L.; Li, W.X.; Yuan, P. Evaluation of site stability of highway passing through goaf based on combined weighting and the cloud matter-element model. *J. Min. Strat. Control Eng.* **2022**, *4*, 63–70.
19. Hao, J.; Sun, Y.F.; Hu, X.H.; Gao, J.; Li HTWang, H.L. Occurrence Characteristics and Stability Evaluation of Old Gob in Abandoned Iron Mine. *Sci. Technol. Eng.* **2023**, *23*, 14154–14162.
20. Guo, Q.B.; Meng, X.R.; Li, Y.M.; Lv, X.; Liu, C. A prediction model for the surface residual subsidence in an abandoned goaf for sustainable development of resource-exhausted cities. *J. Clean. Prod.* **2021**, *279*, 123803. [[CrossRef](#)]
21. Tang, S.; Luo, Z.Q.; Xu, H. Evaluation of Stability of Goaf Based on Fuzzy Matter-element Theory. *China Saf. Sci. J.* **2012**, *22*, 24–30.
22. Zhang, B.; Zhang, L.Z.; Yang, H.L.; Zhang, Z.J.; Tao, J.L. Subsidence prediction and susceptibility zonation for collapse above goaf with thick alluvial cover: A case study of the Yongcheng coalfield, Henan Province, China. *Bull. Eng. Geol. Environ.* **2016**, *75*, 1117–1132. [[CrossRef](#)]
23. Liu, Y.; Eckert, C.M.; Earl, C. A review of fuzzy AHP methods for decision-making with subjective judgements. *Expert Syst. Appl.* **2020**, *161*, 113738. [[CrossRef](#)]
24. Liu, X.M.; Luo, Z.Q.; Yang, C.X.; Zhang, B.; Lu, H. Analysis of stability of cavity based on cavity monitoring. *Rock Soil Mech.* **2007**, *28*, 521–526.
25. Kou, X.Y.; Jia, X.M.; Wang, L.G.; Wu, X. Evaluation and analysis of stability of mined-out area based on the CMS and DIMINE-FLAC3D coupling technique. *Miner. Eng. Res.* **2010**, *25*, 31–35.
26. Yao, Z.W.; Fang, Z.F.; Gui, W.H.; Zheng, G.G.; Wang, L.H. Application of 3D laser scanning technology in goaf detection of Dongguashan copper mine. *Nonferrous Met. (Min. Sect.)* **2020**, *72*, 67–69.
27. Tian, X.; He, R.X.; Zhang, X.; Zhang, X.Y.; Ren, Y.F. Study and Application of Sublevel filling Treatment Scheme for Goaf in Shirengou Iron Mine. *Met. Mine* **2023**, *8*, 162–170.
28. Tian, Z.J.; Nan, S.Q.; Song, A.D. Key Technical Measures in the Early Period of Transition from Open-pit to Underground Mining. *Met. Mine* **2008**, *7*, 27–29+159.
29. Li, L.T.; Yang, Z.Q.; Gao, Q. Experiment on Proportion Optimization of Filling Cementitious Material on Tailings from Shirengou Iron Mine. *Met. Mine* **2016**, *4*, 177–180.
30. Cai, X.S.; Li, S.; Lu, H.J.; Du, Y.N. Optimization of Mining Sequence for Third-stage Underground Ore Body in Shirengou Iron Mine. *Min. Res. Dev.* **2019**, *39*, 61–65.
31. Liu, H.T.; Li, P.T.; Li, J.W.; Li, Z.B. Study on ore body distribution characteristics and ore processing technology performance of Shirengou Iron Mine in Zunhua, Eastern Hebei. *China Energy Environ. Prot.* **2022**, *44*, 58–62.
32. Li, X.; Yu, Q.L.; Yang, T.H.; Dong, X.; Deng, W.X. Risk Analysis of Landslide in Dagushan Open-pit Mine Based on Weighted Information Method. *Met. Mine* **2021**, *2*, 186–193.
33. Qiu, J.X. Evaluation of Mine Geological Environment Based on AHP. *Shandong Coal Sci. Technol.* **2020**, *7*, 178–180+186.

34. Kong, D.Y.; Lu, X.X.; Shen, H.Q.; Yuan, J.; Zhang, Y.R. Optimization evaluation of recycled aggregate production mode based on improved analytic hierarchy process. *J. Zhejiang Univ. Technol.* **2023**, *51*, 504–508.
35. Chen, J.H.; Chen, Y.; Yang, S.; Zhong, X.D.; Han, X. A prediction model on rockburst intensity grade based on variable weight and matter-element extension. *PLoS ONE* **2019**, *14*, e0218525. [[CrossRef](#)]

Disclaimer/Publisher’s Note: The statements, opinions and data contained in all publications are solely those of the individual author(s) and contributor(s) and not of MDPI and/or the editor(s). MDPI and/or the editor(s) disclaim responsibility for any injury to people or property resulting from any ideas, methods, instructions or products referred to in the content.